

Efficient Separation of Monobromotoluene Isomers by Nonporous Adaptive Perbromoethylated Pillar[5]arene Crystals

Bohan Zhao,^{#a} Jianwei Wang,^{#a,b} Li Shao,^d Yitao Wu,^a Ming Li,^{*a} Bin Hua^{*a,b} and Feihe
Huang^{*a,b,c}

^a Stoddart Institute of Molecular Science, Department of Chemistry, Zhejiang University,
Hangzhou 310058, P. R. China; Fax and Tel: +86-571-8795-3189. Email addresses:
mingzhelee@zju.edu.cn; huabin@zju.edu.cn; fhuang@zju.edu.cn

^b Zhejiang-Israel Joint Laboratory of Self-Assembling Functional Materials, ZJU-Hangzhou
Global Scientific and Technological Innovation Center, Zhejiang University, Hangzhou
311215, P. R. China

^c Green Catalysis Center and College of Chemistry, Zhengzhou University, Zhengzhou
450001, P. R. China

^d Department of Materials Science and Engineering, Zhejiang Sci-Tech University, Hangzhou
310018, P. R. China

Electronic Supplementary Information (33 pages)

1. Materials	S2
2. Methods	S3
3. Crystallographic Data	S5
4. Characterization of Activated Pillararene Crystals.....	S7
5. Vapor-Phase Adsorption Measurements	S12
6. Recyclability Test	S29
7. References	S33

1. Materials

All the starting materials including *o*-bromotoluene (**OBT**) and *m*-bromotoluene (**MBT**) were purchased and used as received. Perbromoethylated pillararenes (**BrP5** and **BrP6**) were synthesized as described previously.^{S1,S2} Activated **BrP5** and **BrP6** were prepared according to reported procedures.^{S3}

Table S1. Physical properties of **OBT** and **MBT**.

Compound	Melting Point (K)	Boiling Point (K)	Saturated Vapor Pressure at 298 K (mm Hg)
OBT	246.15	453.95	1.2 ± 0.3
MBT	233.15	455.25	1.1 ± 0.3
PBT	301.65	456.95	1.0 ± 0.3

2. Methods

2.1. Powder X-Ray Diffraction

X-ray powder diffraction data were measured on a SmartLab diffractometer with fixed divergence slits and a D/tex Ultra 250 detector at room temperature. The diffractometer was configured in parafocusing Bragg-Brentano geometry. Data was collected over a 2-theta range of 5° to 45° with a step size of 0.02° and a scan rate of 5°/min using a Cu K_{α} radiation at a powder of 40 kV and 180 mA. Cu K_{β} radiation was removed using a divergent beam Ni filter.

2.2. Thermogravimetric Analysis

TGA was carried out using a Q5000IR analyzer (TA Instruments) with an automated vertical overhead thermobalance. The samples were heated at 10 °C/min using N₂ as the protective gas.

2.3. Single Crystal Growth

Single crystals of guest-loaded **BrP6** were grown by volatilization: A quantity of 5.00 mg of **BrP6** powder in its dried form was carefully dispensed into a small vial where 1.00 mL of the guest was added and the vial was heated until all the powder was dissolved. Colorless crystals were got by volatilization for 2-15 days.

2.4. Single Crystal X-ray Diffraction

Single crystal X-ray diffraction data were collected on a Bruker D8 VENTURE CMOS X-ray diffractometer with graphite monochromatic Mo- K_{α} radiation ($\lambda = 0.71073 \text{ \AA}$).

2.5. Solution ¹H NMR Spectroscopy

¹H NMR spectra were recorded by using a Bruker Avance DMX 600 spectrometer.

2.6. Gas Chromatography

Gas chromatographic analysis: GC measurements were carried out using an Agilent 7890B instrument configured with an FID detector and a HP-chiral β column (30 m \times 0.32 mm \times 0.25 μ m). Samples were analyzed using headspace injections and were performed by incubating the sample at 85 °C for 30 min followed by sampling 1.00 mL of the headspace. The total volume of the container is 10 mL; the mass of the solid in the container is about 10 mg; the total volume of the headspace is 1 mL.

3. Crystallographic Data

Table S2. Experimental single crystal X-ray data for **(OBT)₂@BrP6**.

Collection Temperature [K]	170.00
Formula	C ₈₀ H ₈₆ Br ₁₄ O ₁₂
Crystal System	monoclinic
Space Group	<i>P2₁/c</i>
<i>a</i> [Å]	25.7704(16)
<i>b</i> [Å]	13.7621(10)
<i>c</i> [Å]	23.8060(17)
α [°]	90
β [°]	90.1300(5)
γ [°]	90
Volume [Å ³]	8442.9(10)
<i>Z</i>	4
<i>D</i> _{calcd} [g cm ⁻³]	1.855
μ [mm ⁻¹]	6.697
F(000)	4608.0
Crystal size [mm ³]	0.23 × 0.13 × 0.06
Radiation	MoK α ($\lambda = 0.71073$)
2θ range [°]	3.77 to 55.123
Index ranges	$-33 \leq h \leq 33,$ $-17 \leq k \leq 17,$ $-30 \leq l \leq 30$
Reflections collected	128129
Independent reflections	19153 [$R_{int} = 0.1427,$ $R_{sigma} = 0.1004$]
Data/restraints/parameters	19153/1066/1152

Goodness-of-fit on F^2	1.035
Final R indexes [$I > 2\sigma(I)$]	$R_1 = 0.1014,$ $wR_2 = 0.2582$
Final R indexes [all data]	$R_1 = 0.1579,$ $wR_2 = 0.2943$
Largest diff. peak/hole / $e \text{ \AA}^{-3}$	3.01/-1.52
CCDC	2261922

4. Characterization of Activated Pillararene Crystals

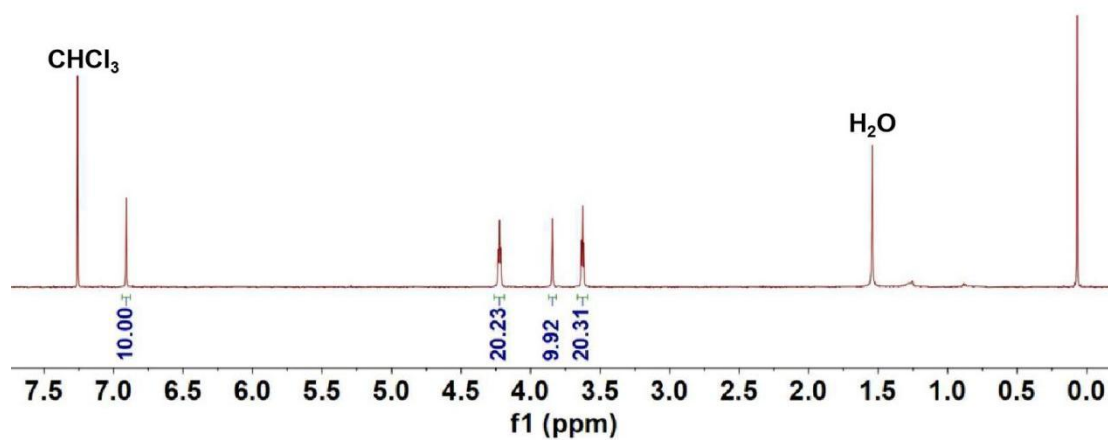


Fig. S1 ¹H NMR spectrum (600 MHz, chloroform-*d*, 298 K) of activated **BrP5** crystals.

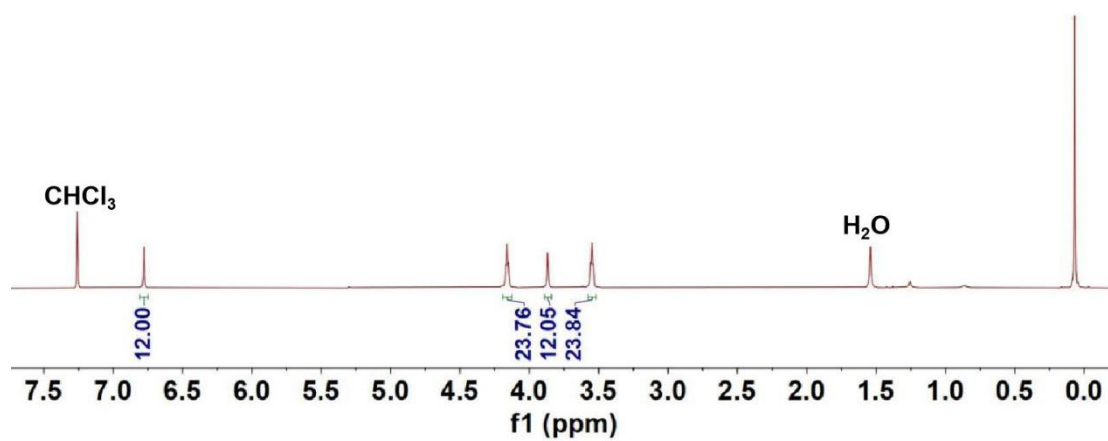


Fig. S2 ¹H NMR spectrum (600 MHz, chloroform-*d*, 298 K) of activated **BrP6** crystals.

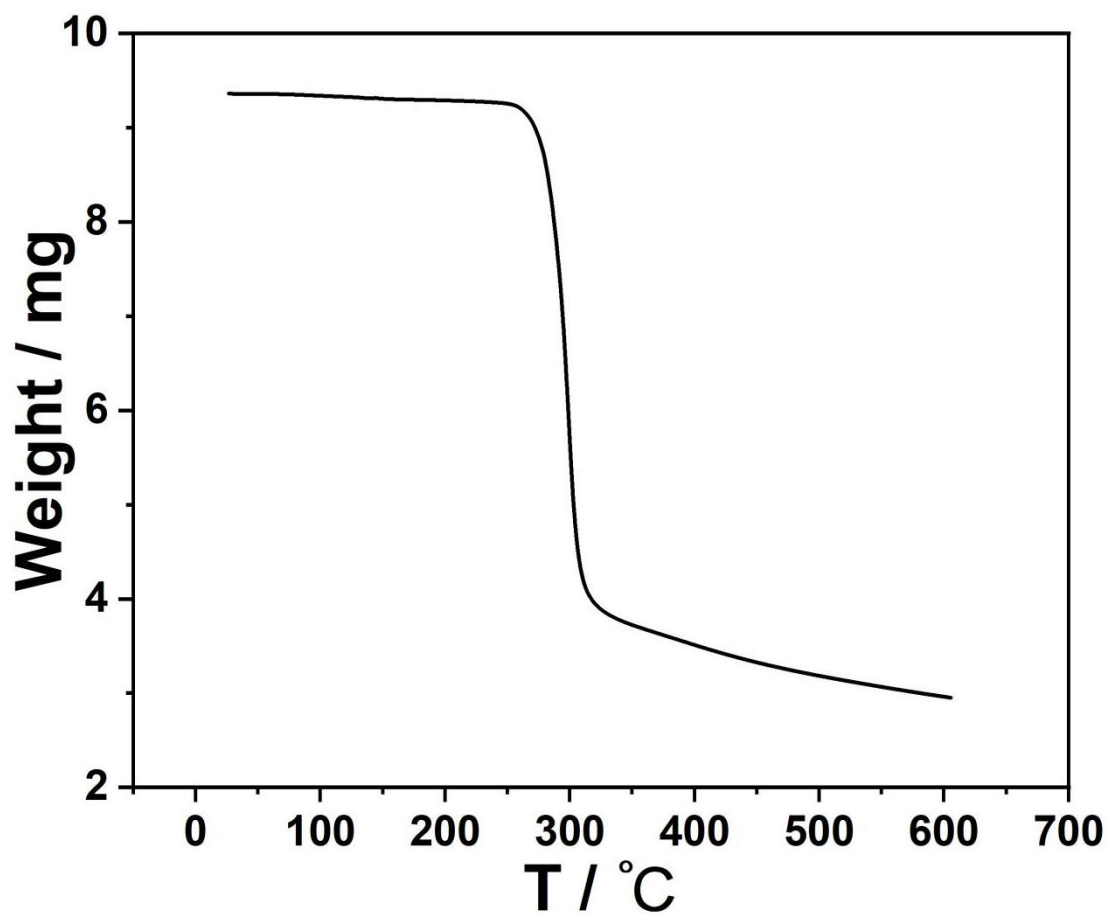


Fig. S3 Thermogravimetric analysis of activated **BrP5** crystals.

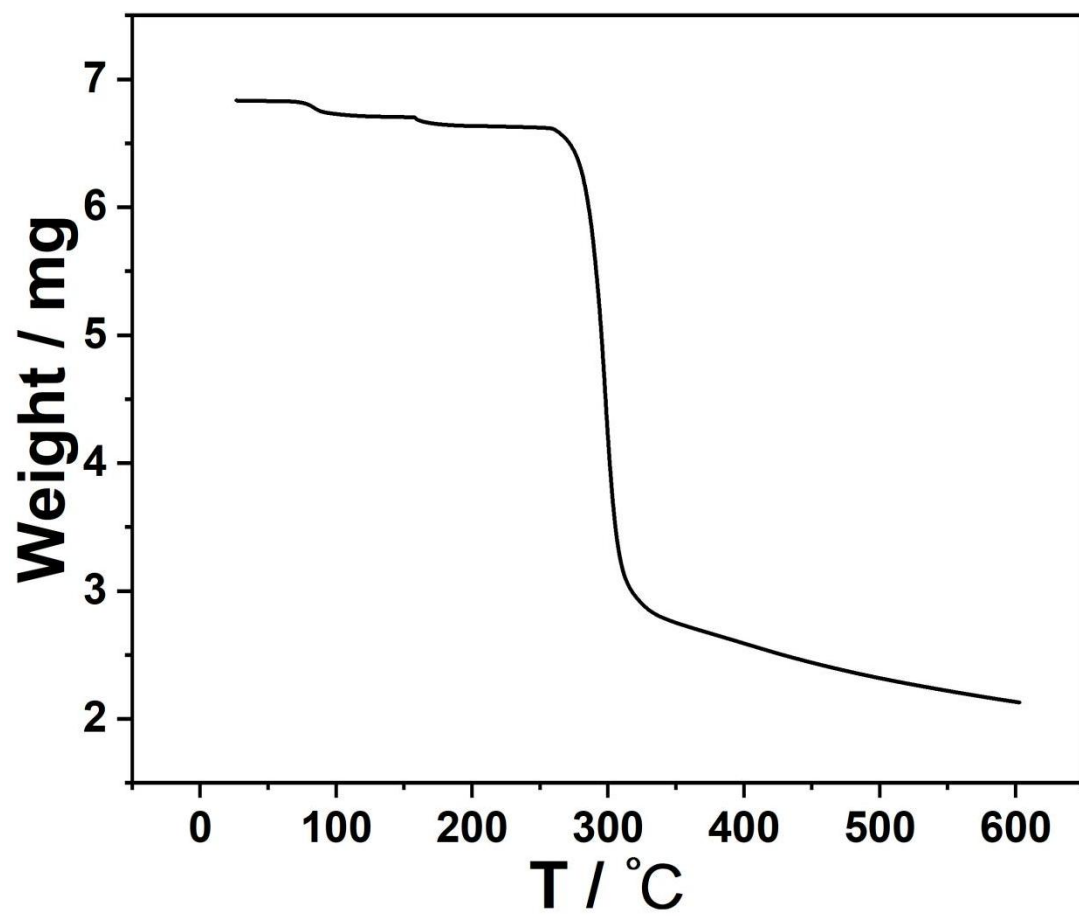


Fig. S4 Thermogravimetric analysis of activated **BrP6** crystals.

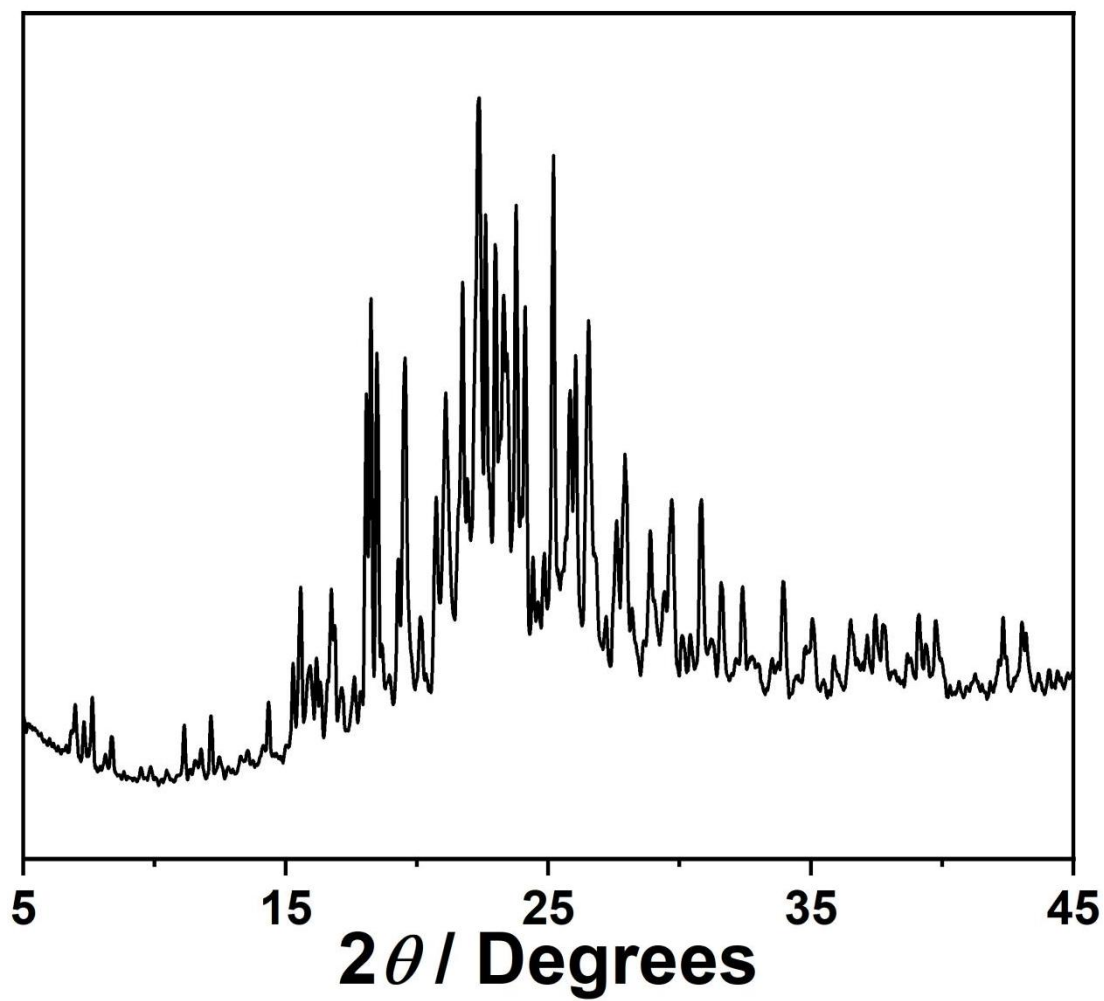


Fig. S5 Powder X-ray diffraction pattern of activated **BrP5** crystals.

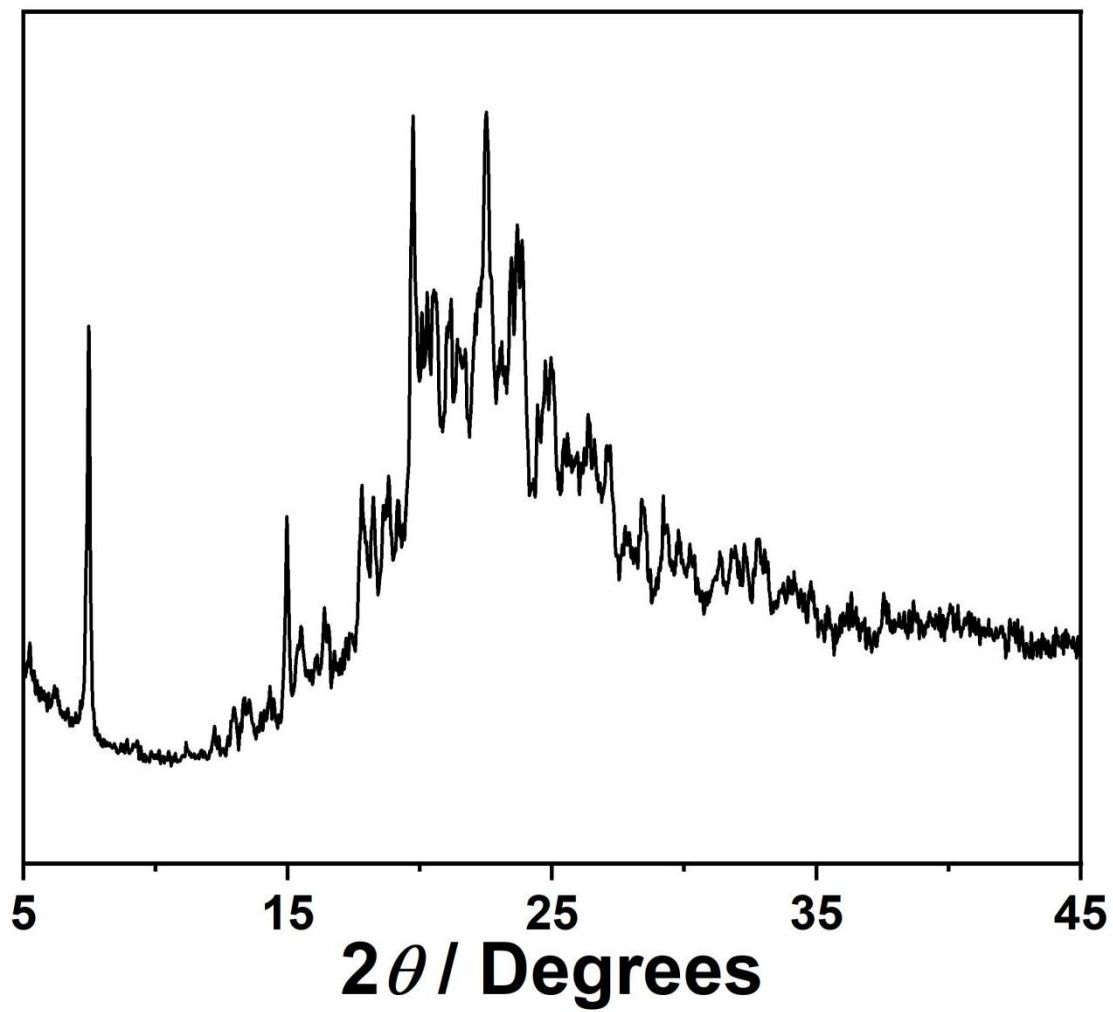


Fig. S6 Powder X-ray diffraction pattern of activated **BrP6** crystals.

5. Vapor-Phase Adsorption Measurements

5.1. Single-Component Monobromotoluene Isomers Adsorption Experiments

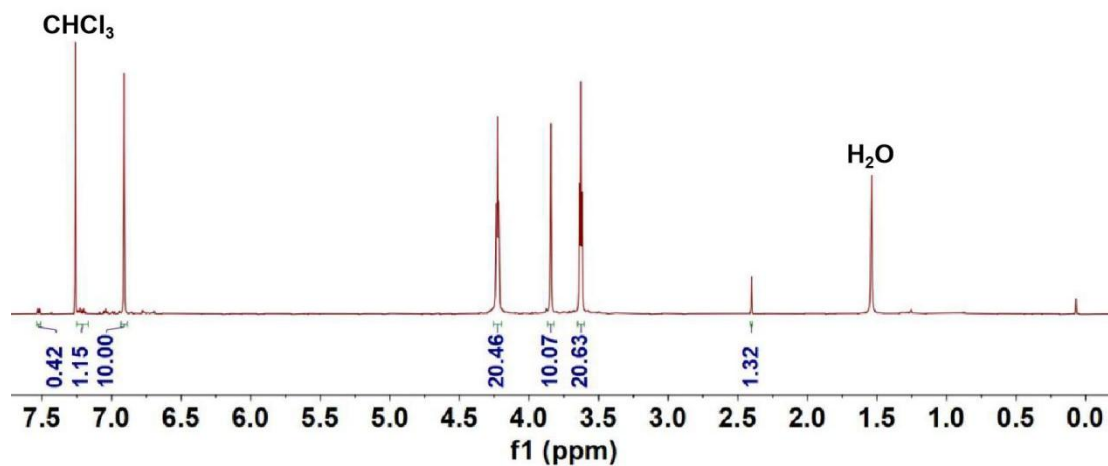


Fig. S7 ¹H NMR spectrum (600 MHz, chloroform-*d*, 298 K) of activated **BrP5** crystals after adsorption of **OBt** vapor. The integration can be calculated as 0.44 equiv. of **OBt** per **BrP5** molecule.

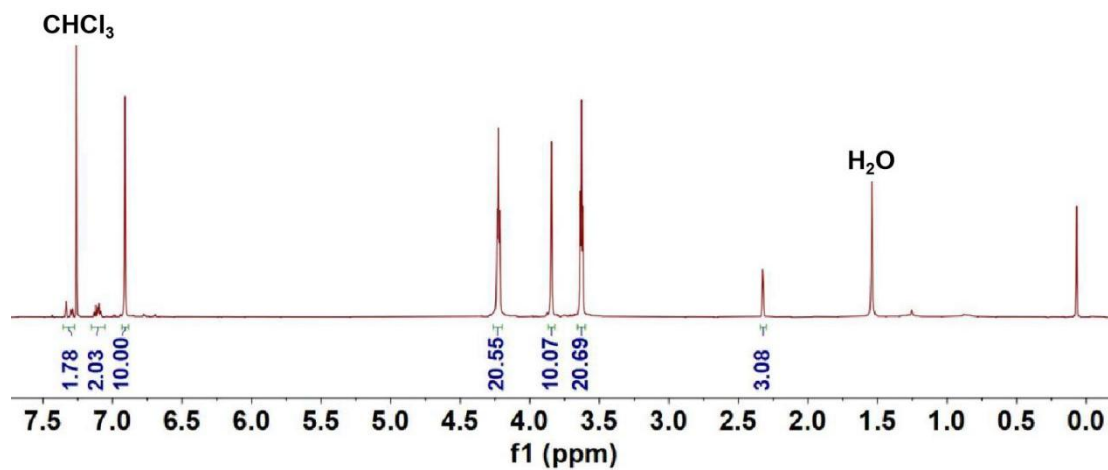


Fig. S8 ¹H NMR spectrum (600 MHz, chloroform-*d*, 298 K) of activated **BrP5** crystals after adsorption of **MBT** vapor. The integration can be calculated as 1.03 equiv. of **MBT** per **BrP5** molecule.

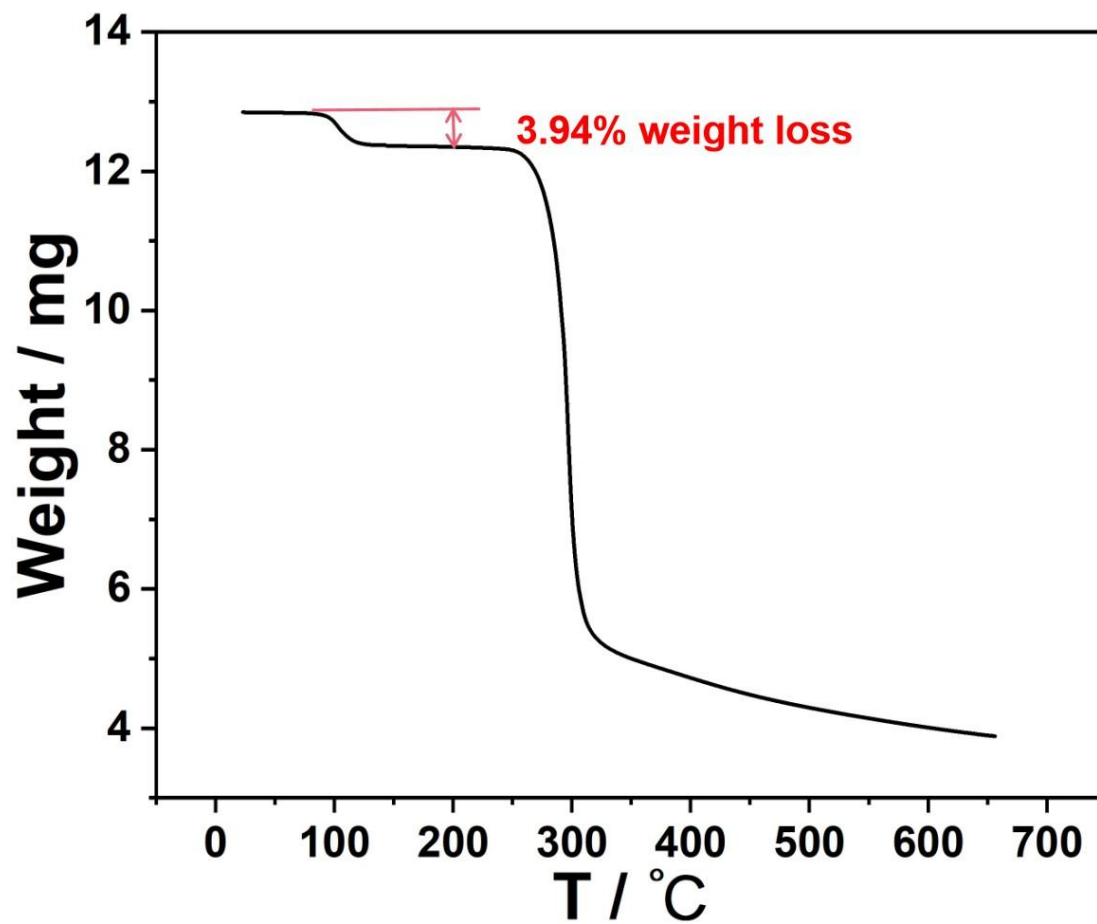


Fig. S9 Thermogravimetric analysis of activated **BrP5** crystals after adsorption of **OBT** vapor. The weight loss below 100 °C can be calculated as about 0.4 equiv. of **OBT** per **BrP5** molecule.

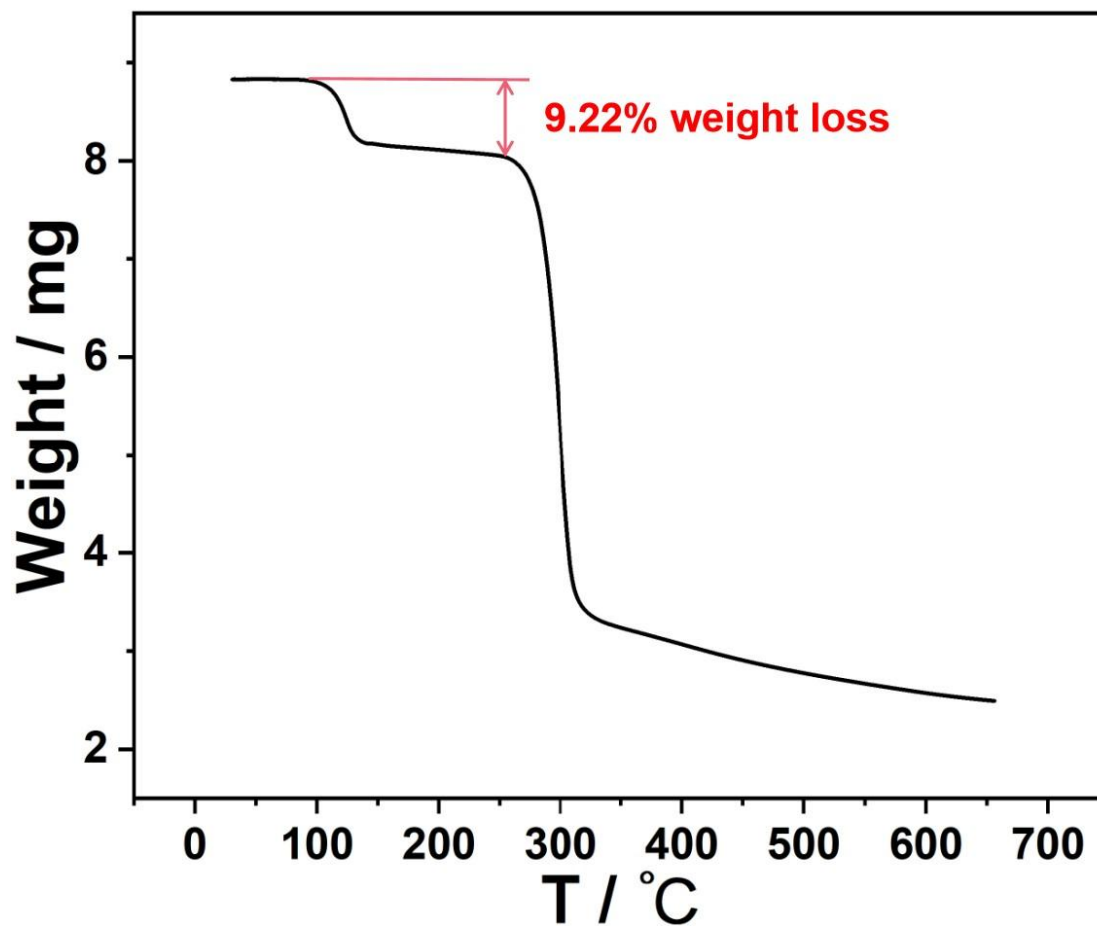


Fig. S10 Thermogravimetric analysis of activated **BrP5** crystals after adsorption of **MBT** vapor. The weight loss below 100 °C can be calculated as about 1.0 equiv. of **MBT** per **BrP5** molecule.

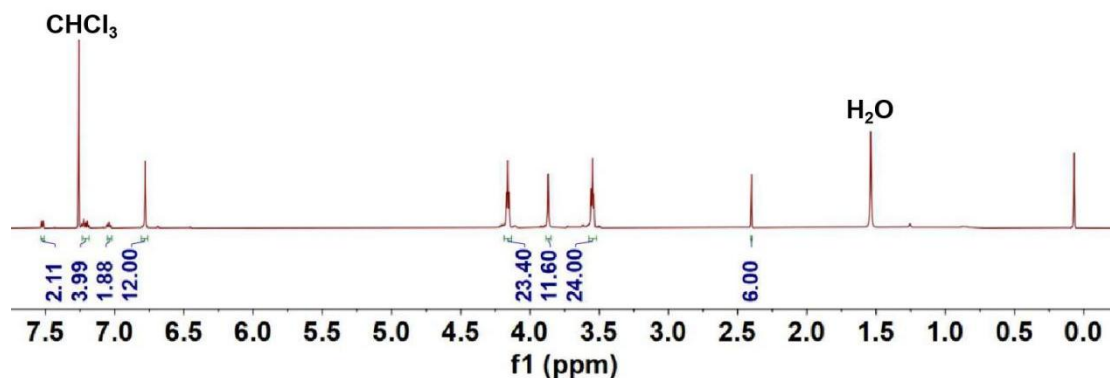


Fig. S11 ¹H NMR spectrum (600 MHz, chloroform-*d*, 298 K) of activated **BrP6** crystals after adsorption of **OBT** vapor. The integration can be calculated as 2.00 equiv. of **OBT** per **BrP6** molecule.

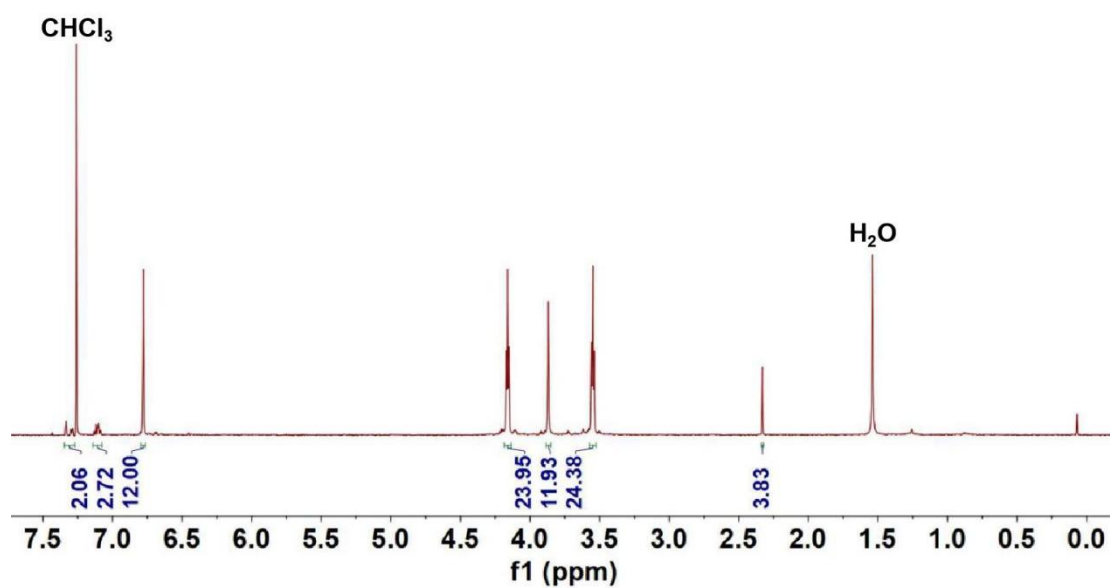


Fig. S12 ¹H NMR spectrum (600 MHz, chloroform-*d*, 298 K) of activated **BrP6** crystals after adsorption of **MBT** vapor. The integration can be calculated as 1.28 equiv. of **MBT** per **BrP5** molecule.

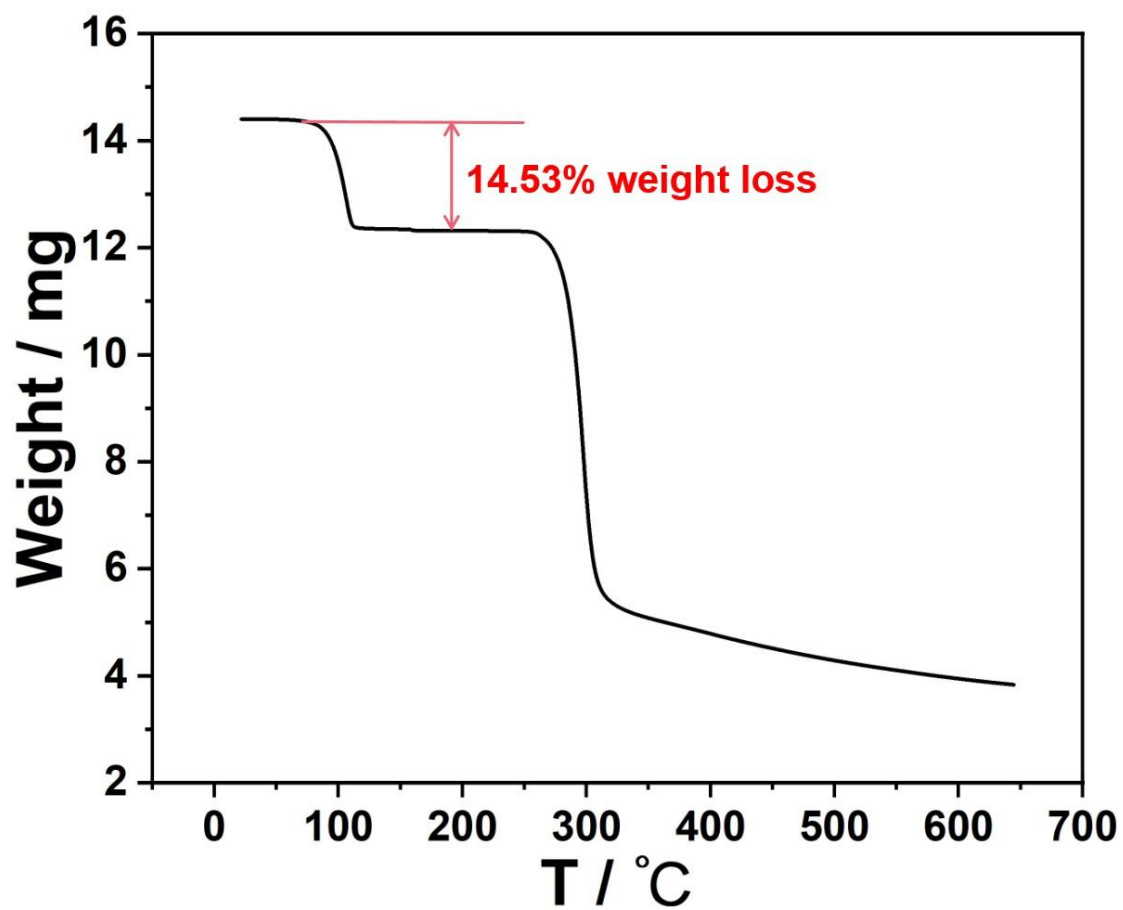


Fig. S13 Thermogravimetric analysis of activated **BrP6** crystals after adsorption of **OBT** vapor. The weight loss below 100 °C can be calculated as about 2.0 equiv. of **OBT** per **BrP6** molecule.

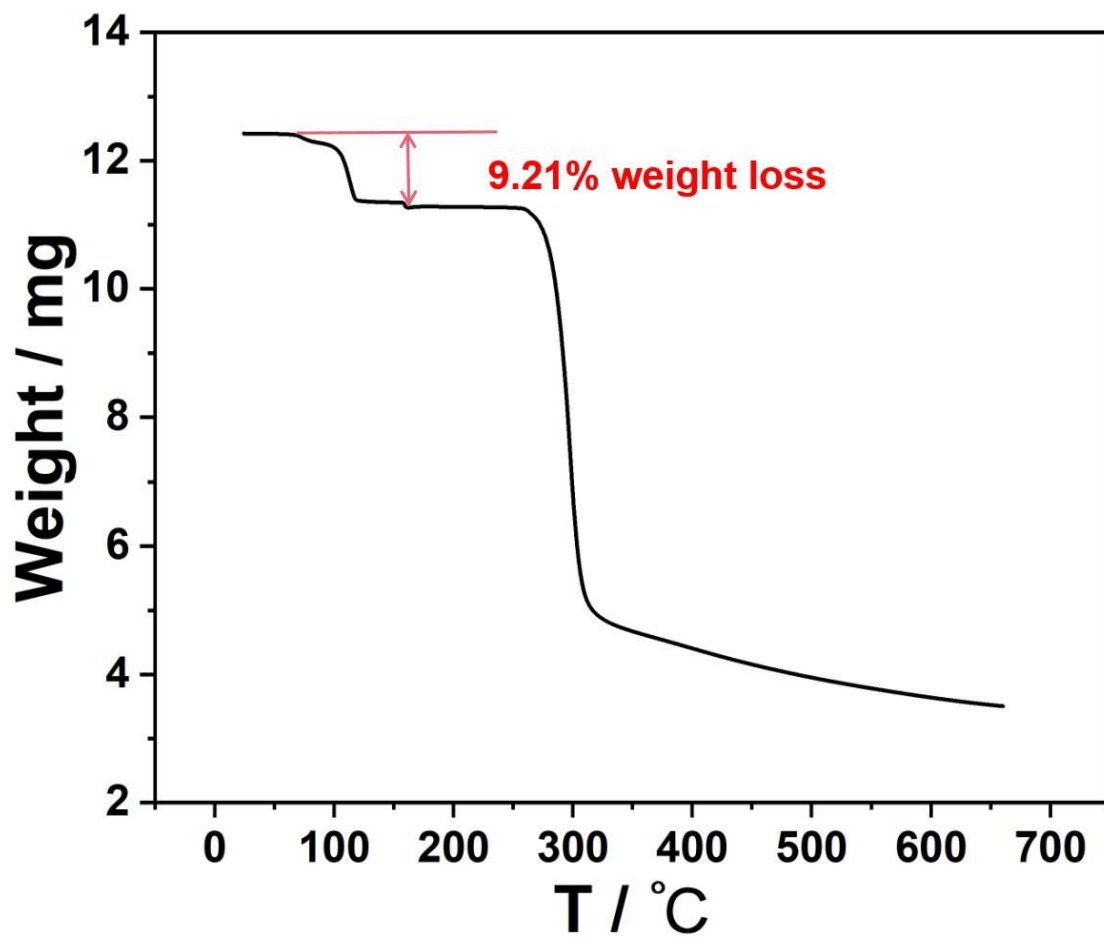


Fig. S14 Thermogravimetric analysis of activated **BrP6** crystals after adsorption of **MBT** vapor. The weight loss below 100 °C can be calculated as about 1.2 equiv. of **MBT** per **BrP5** molecule.

5.2. Structural Analyses

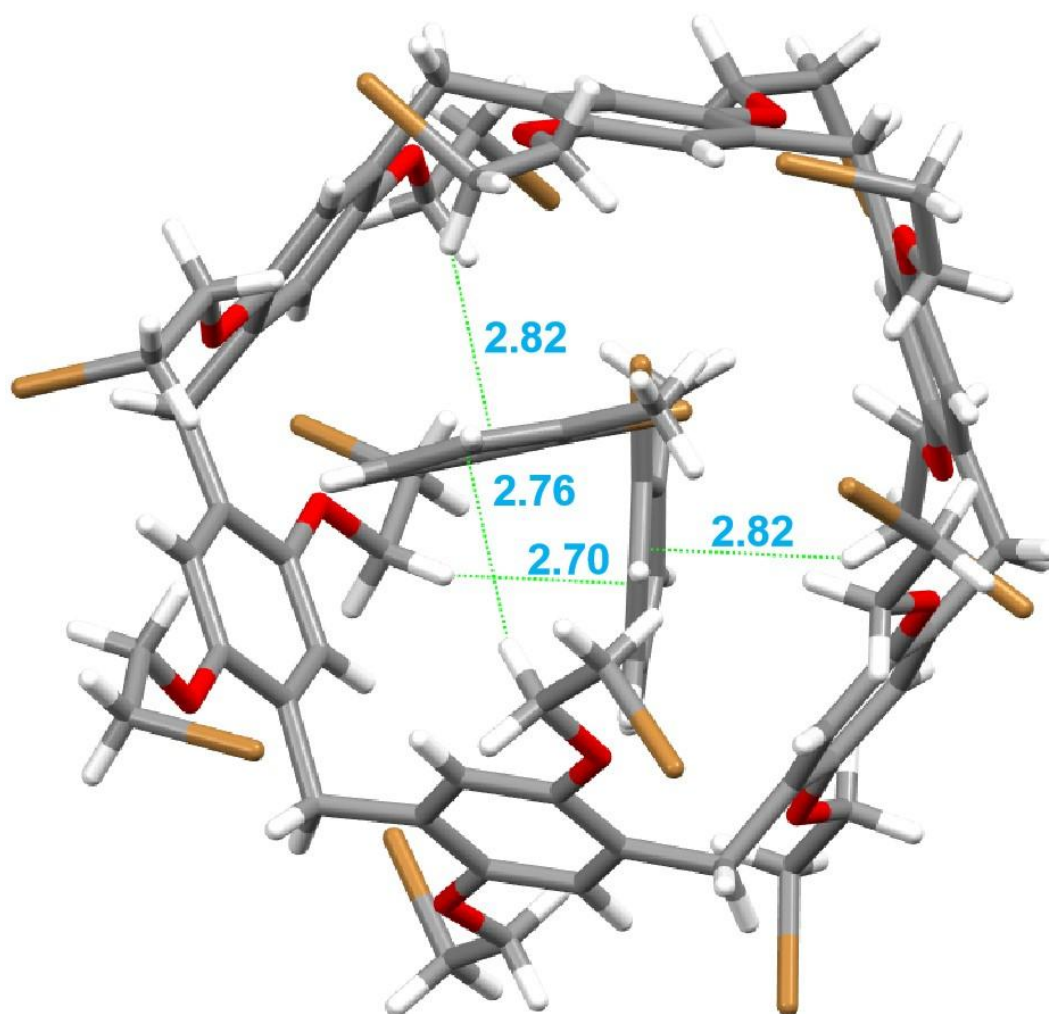


Fig. S15 Single crystal structure of **(OBT)₂@BrP6**. [C–H··· π] distances (Å): 2.70; 2.76; 2.82; 2.82.

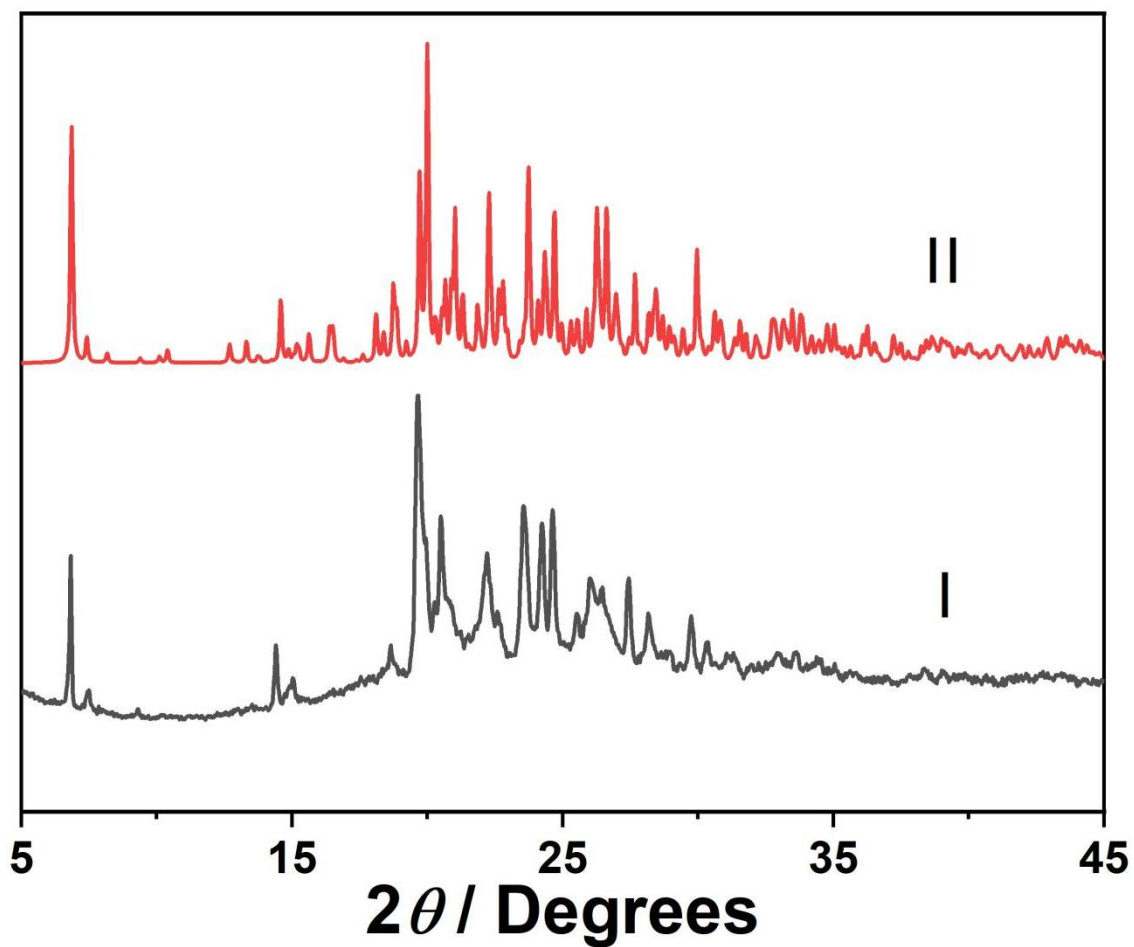


Fig. S16 Powder X-ray diffraction patterns of **BrP6**: (I) after adsorption of **OBT** vapor; (II) simulated from single crystal structure of **(OBT)₂@BrP6**.

Moreover, we investigated the integration ability of **BrP5** with **MBT** by Job plot and ^1H NMR titration according to the previous report.^{S4} The Job plot illustrated that the binding stoichiometry is 1:1 for **BrP5** and **MBT** in CDCl_3 (Fig. S17). ^1H NMR titration experiment demonstrated that the binding constant (K) of **BrP5** and **MBT** was $6.01 \pm 0.48 \text{ M}^{-1}$ (Fig. S18).

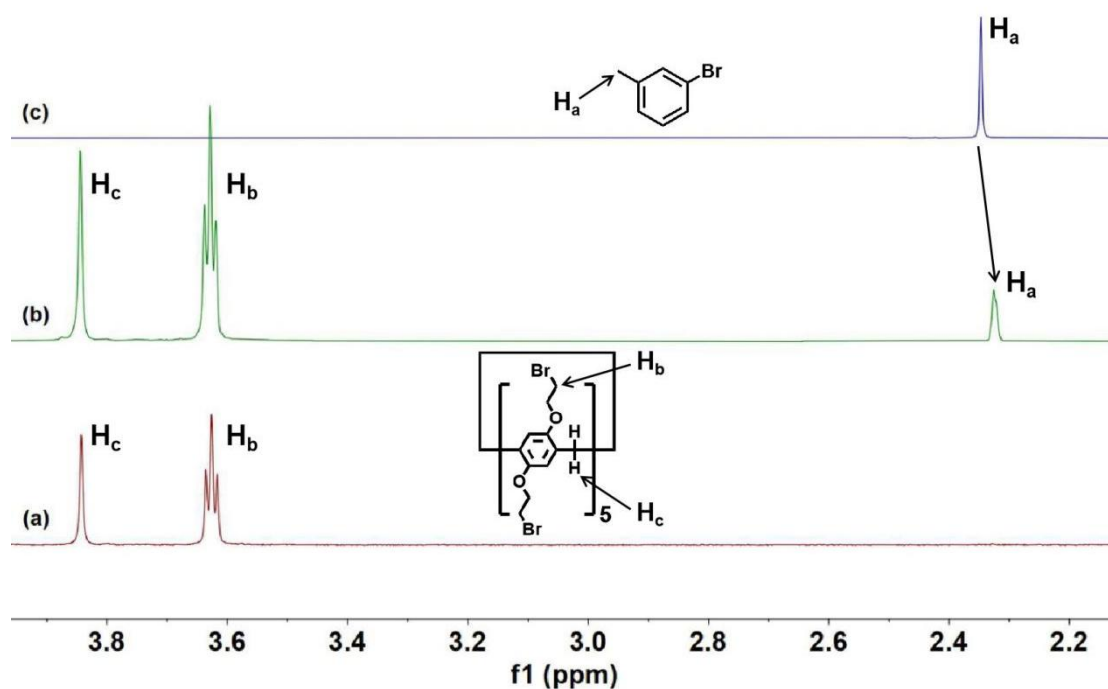


Fig. S17 ^1H NMR spectra (600 MHz, chloroform-*d*, 298 K): (a) **BrP5**; (b) **BrP5** after adsorbing **MBT**; (c) **MBT**. The peaks of **MBT** displayed upfield shifts in spectrum (b), indicating that **MBT** was located in the cavity of **BrP5** in solution.

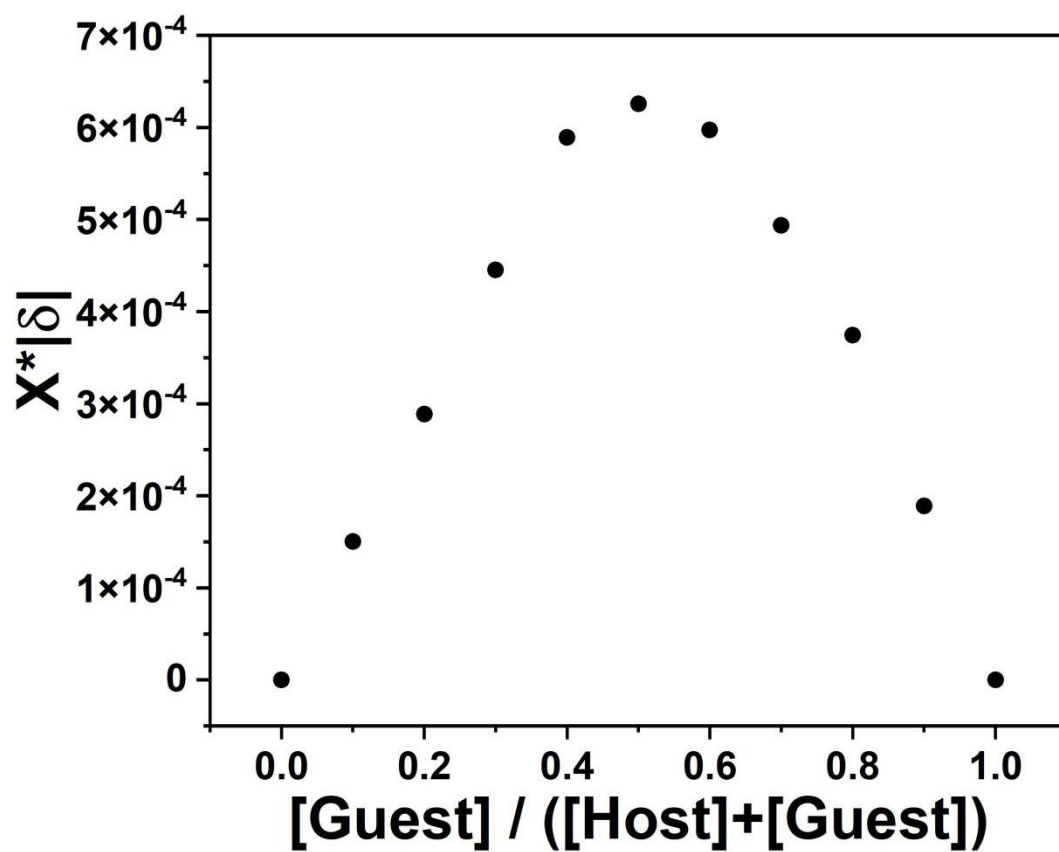


Fig. S18 Job plot showing the 1:1 stoichiometry of the complexation between BrP5 and MBT in CDCl₃.



Fig. S19 A plot of the resonance downfield shifts of H₁, H₂ and H₃ of **BrP5** versus $[\text{MBT}] / [\text{BrP5}]$. The data were fitted to a 1:1 binding model to give $K = 6.01 \pm 0.48 \text{ M}^{-1}$. All solid lines were obtained from non-linear curve-fitting to a 1:1 binding model using the www.supramolecular.org web applet.

5.3. The adsorption behavior of **BrP6** to an equal volume **MBT** and **OBT** mixture

For each vapor-phase mixture experiment, an open 5.00 mL vial containing 20.00 mg of activated **BrP6** adsorbent was placed in a sealed 20.00 mL vial containing 1.00 mL of a 50:50 *v/v* **MBT** and **OBT** mixture. The relative uptake of **MBT** or **OBT** by activated **BrP6** was measured by heating the crystals to release the adsorbed vapor using gas chromatography. Before measurements, the crystals were heated at 60 °C for half an hour to remove the surface-physically adsorbed vapor.

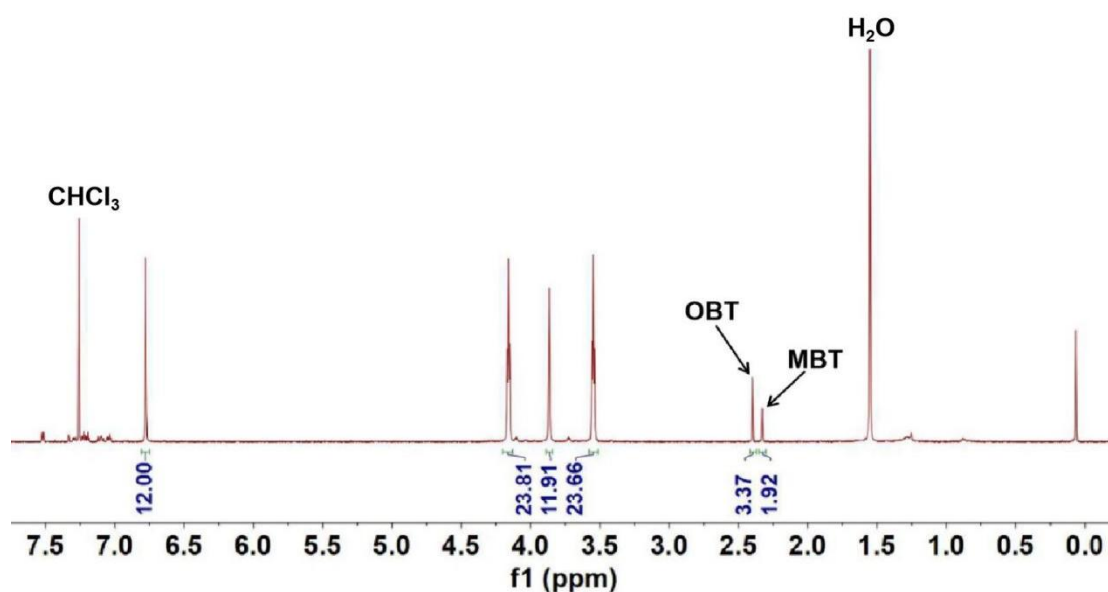


Fig. S20 ¹H NMR spectrum (600 MHz, chloroform-*d*, 298 K) of activated **BrP6** crystals after adsorption of a 50:50 (*v/v*) **MBT** and **OBT** mixture vapor.

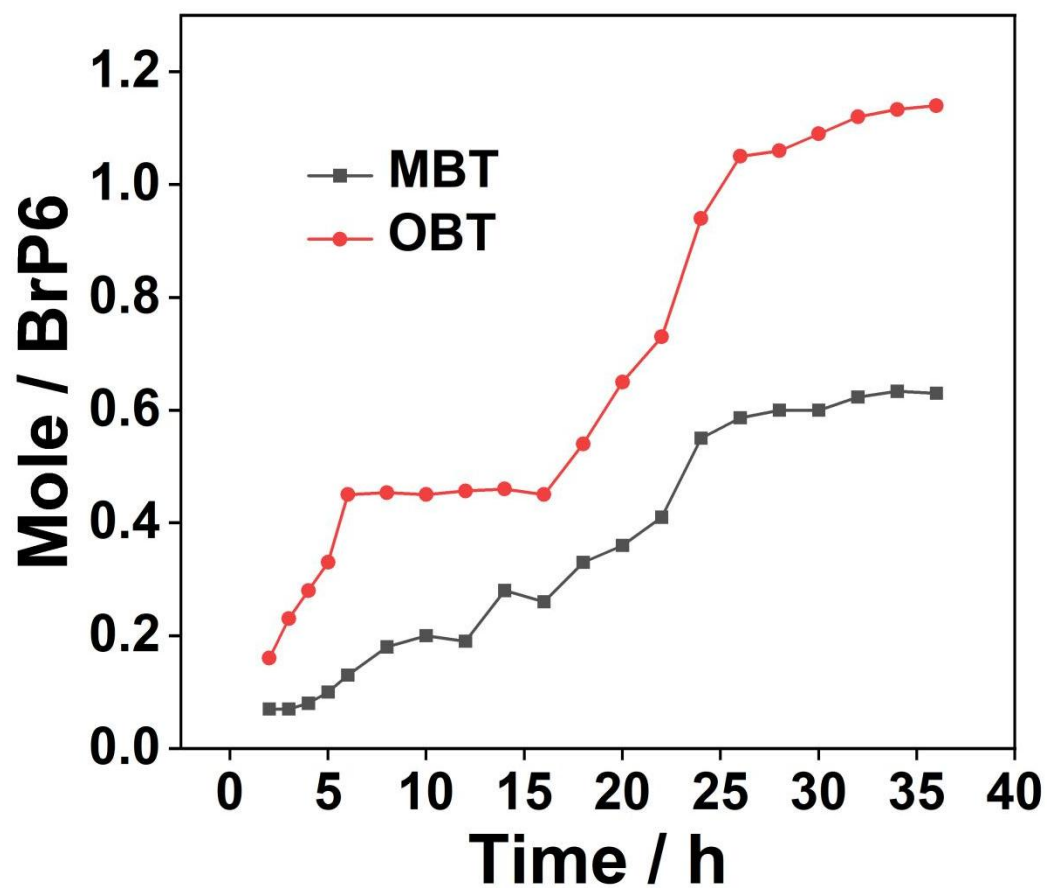


Fig. S21 Time-dependent solid-vapor adsorption plots of **BrP6** for **MBT** and **OBT** (v:v = 50:50) mixed vapor at 303 K.

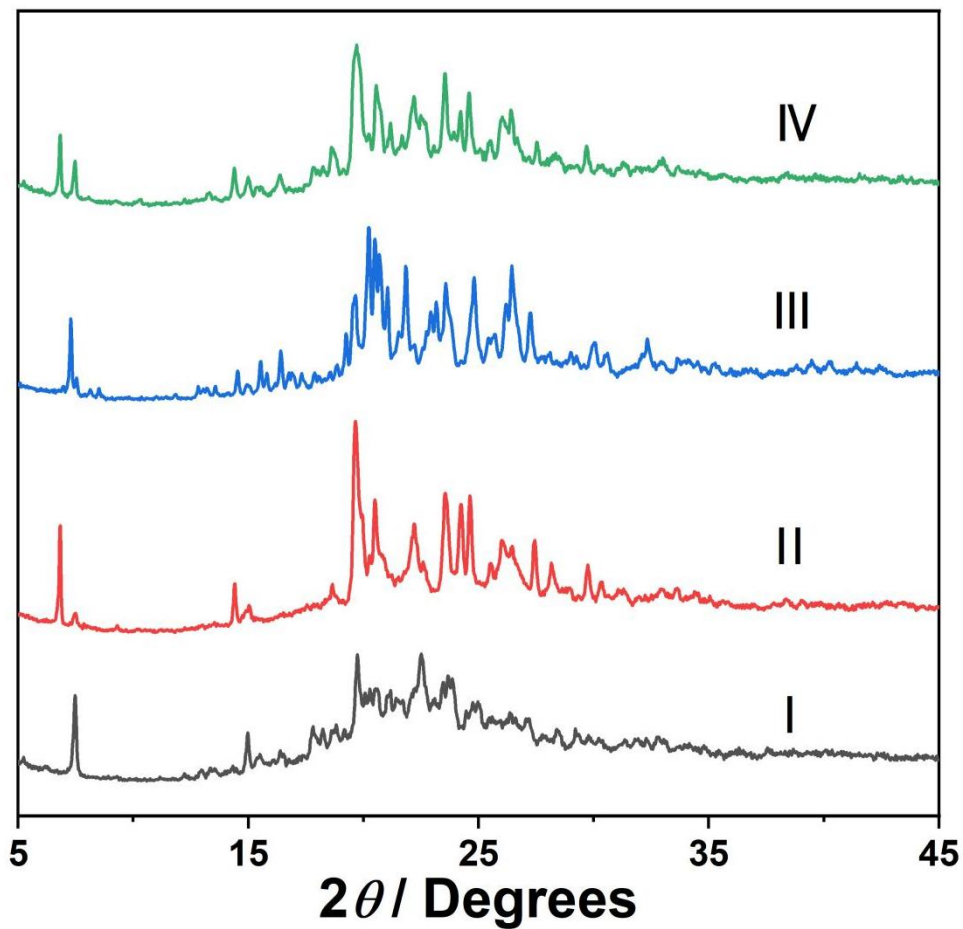


Fig. S22 Powder X-ray diffraction patterns of **BrP6** crystals: (I) original activated **BrP6** crystals; (II) after adsorption of **OBT** vapor; (III) after adsorption of **MBT** vapor; (IV) after exposure to **MBT** and **OBT** equal volume mixture vapor. The pattern of (IV) resembled the superposition of (II) and (III).

5.4. The adsorption behavior of **BrP5** to an equal volume **MBT** and **OBT** mixture

For each vapor-phase mixture experiment, an open 5.00 mL vial containing 20.00 mg of activated **BrP5** adsorbent was placed in a sealed 20.00 mL vial containing 1.00 mL of a 50:50 *v/v* **MBT** and **OBT** mixture. The relative uptake of **MBT** or **OBT** by activated **BrP5** was measured by heating the crystals to release the adsorbed vapor using gas chromatography. Before measurements, the crystals were heated at 60 °C for half an hour to remove the surface-physically adsorbed vapor.

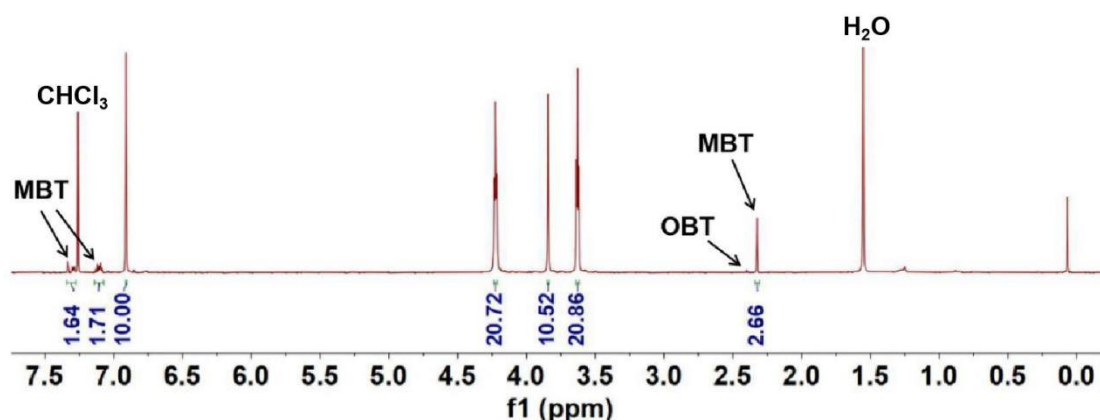


Fig. S23 ¹H NMR spectrum (600 MHz, chloroform-*d*, 298 K) of activated **BrP5** crystals after adsorption of a 50:50 *v/v* **MBT** and **OBT** mixture vapor.

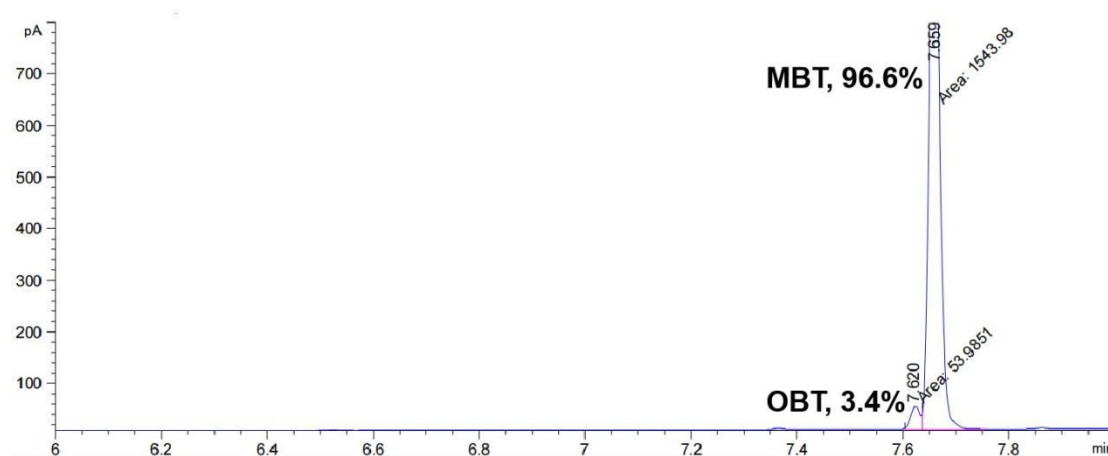


Fig. S24 Relative uptake of the **MBT/OBT** mixture (*v:v* = 50:50) adsorbed in activated **BrP5** crystals after 40 hours.

5.5. The adsorption behavior of **BrP5** to different volume **MBT** and **OBT** mixtures

For each vapor-phase mixture experiment, an open 5.00 mL vial containing 20.00 mg of activated **BrP5** adsorbent was placed in a sealed 20.00 mL vial containing 1.00 mL of different volume **MBT** and **OBT** mixtures. The volume ratios of **MBT** and **OBT** were 20:80, 40:60, 60:40, 80:20, respectively. The relative uptake of **MBT** or **OBT** by activated **BrP5** was measured by heating the crystals to release the adsorbed vapor using gas chromatography. Before measurements, the crystals were heated at 60 °C for half an hour to remove the surface-physically adsorbed vapor.

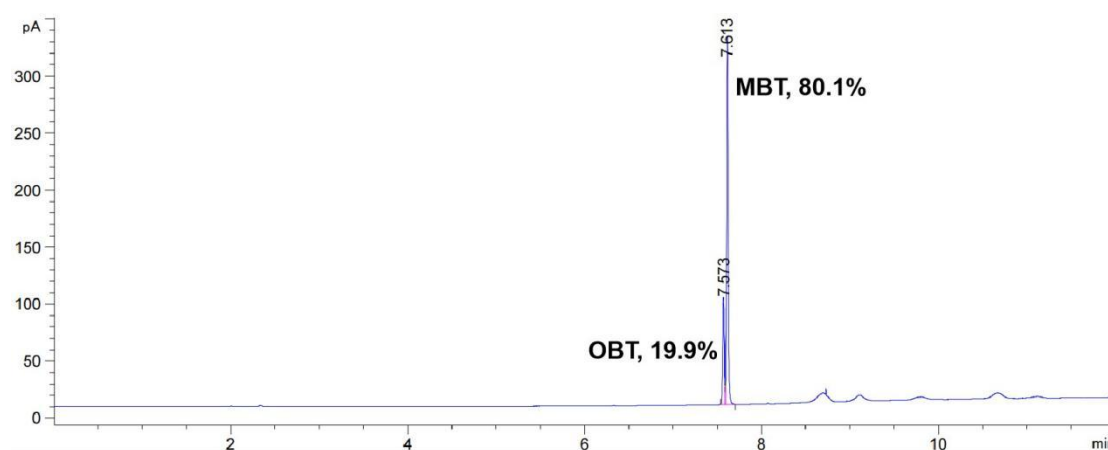


Fig. S25 Relative uptake of the **MBT/OBT** mixture (v:v = 20:80) adsorbed in activated **BrP5** crystals after 40 hours.

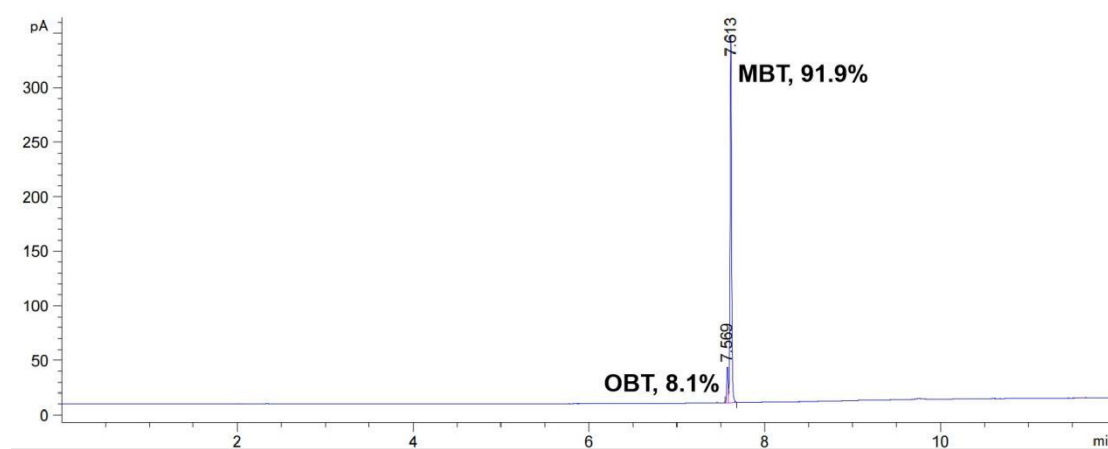


Fig. S26 Relative uptake of the **MBT/OBT** mixture (v:v = 40:60) adsorbed in activated **BrP5** crystals after 40 hours.

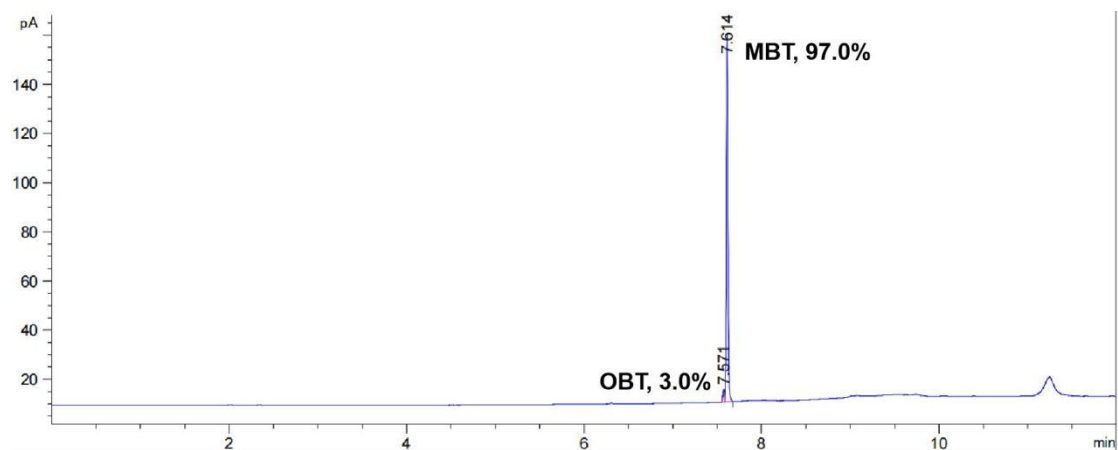


Fig. S27 Relative uptake of the MBT/OBT mixture (v:v = 60:40) adsorbed in activated BrP5 crystals after 40 hours.

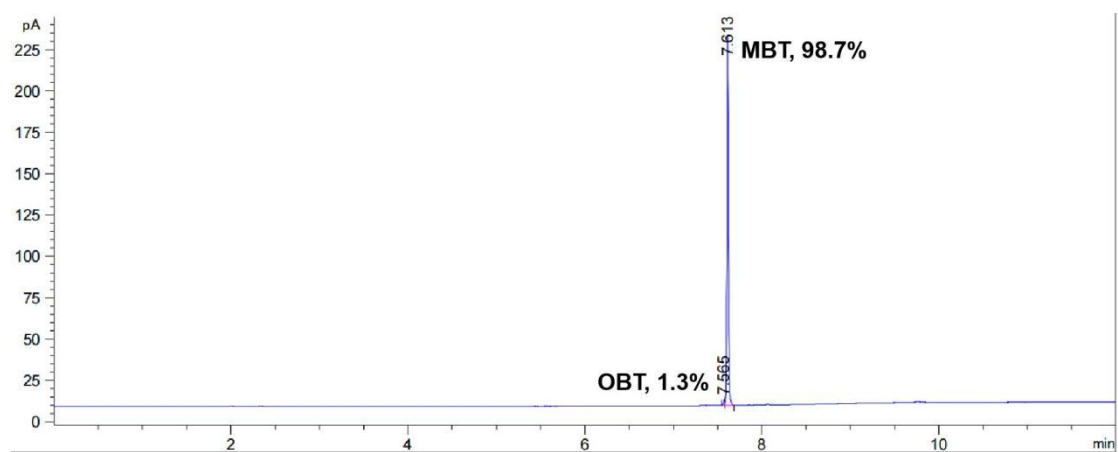


Fig. S28 Relative uptake of the MBT/OBT mixture (v:v = 80:20) adsorbed in activated BrP5 crystals after 40 hours.

6. Recyclability Test

Recyclability of Activated **BrP5** Crystals

An open 5.00 mL vial containing 20.00 mg of **BrP5** after adsorption was desolvated under vacuum at 100 °C overnight. The resultant crystals were characterized by PXRD and ¹H NMR.

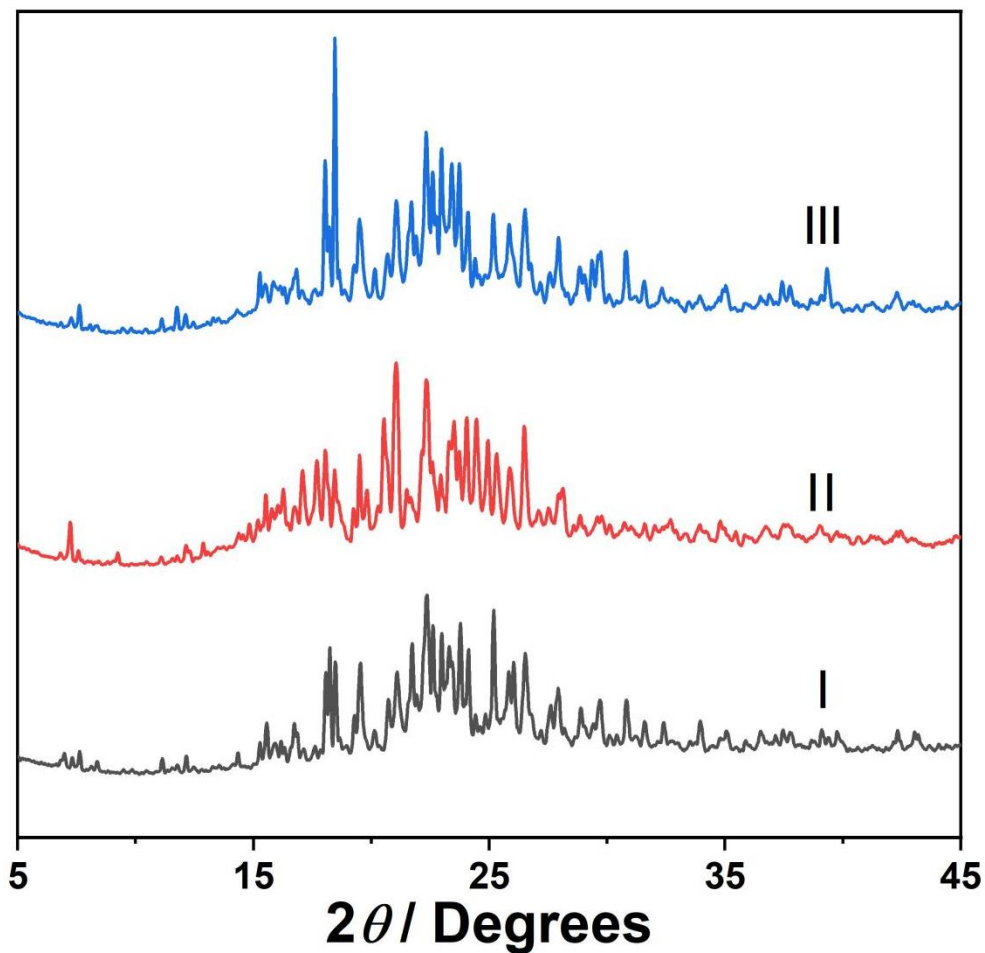


Fig. S29 Powder X-ray diffraction patterns of **BrP5** crystals: (I) original activated **BrP5** crystals; (II) **BrP5** crystals after exposure to **MBT** and **OBT** equal volume mixture vapor; (III) desolvated **BrP5** crystals.

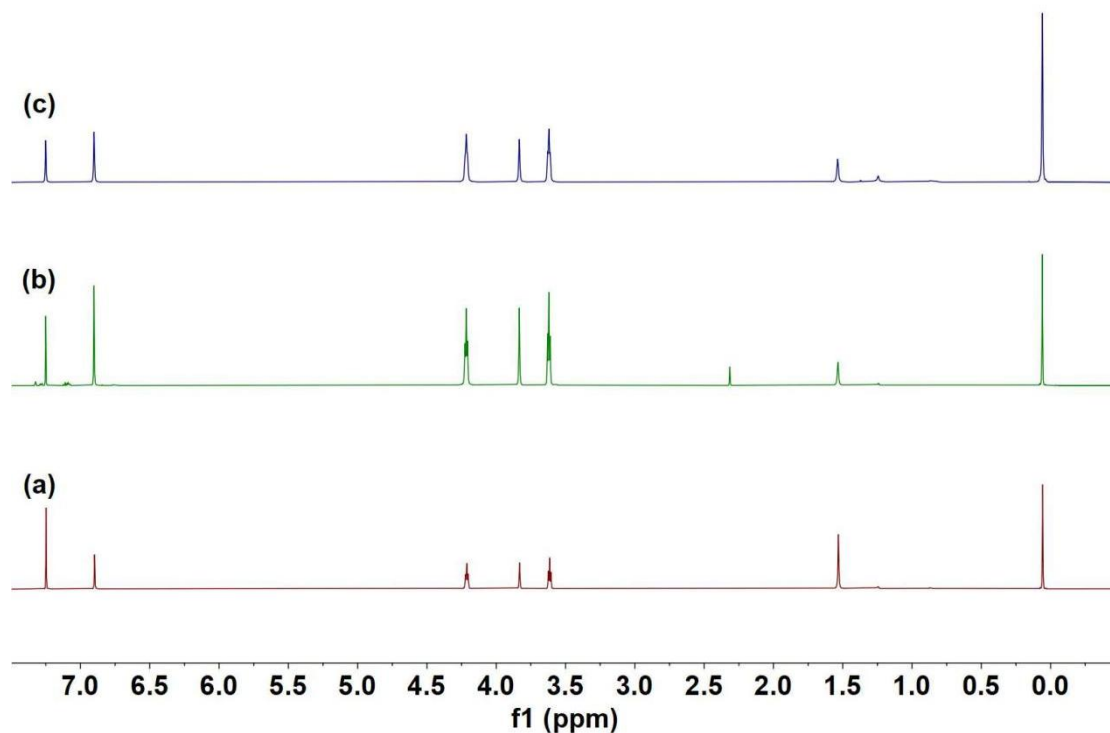


Fig. S30 ^1H NMR spectra (600 MHz, chloroform-*d*, 298 K): (a) original activated **BrP5** crystals; (b) **BrP5** crystals after exposure to **MBT** and **OBT** equal volume mixture vapor; (c) desolvated **BrP5** crystals.

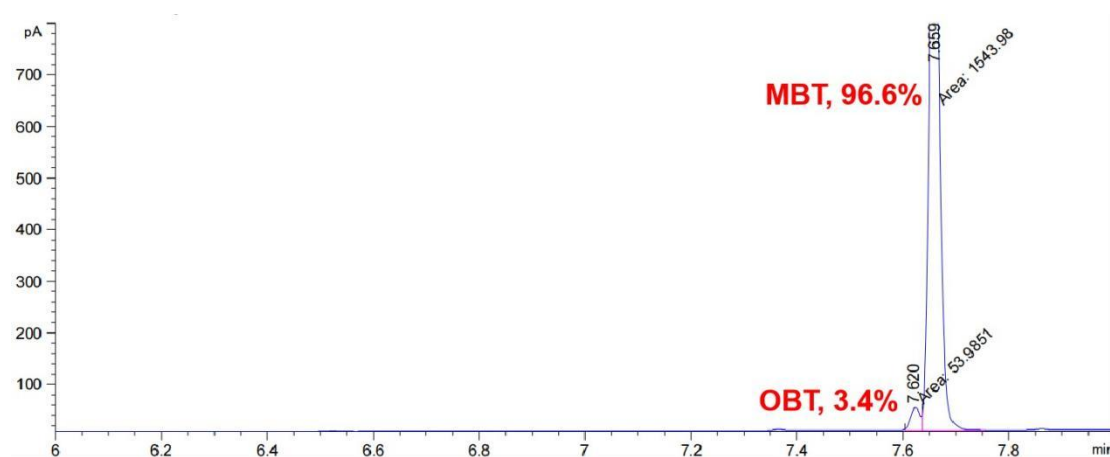


Fig. S31 The first cycle of adsorption of the equal volume mixture of **MBT** and **OBT** by **BrP5** crystals measured by GC.

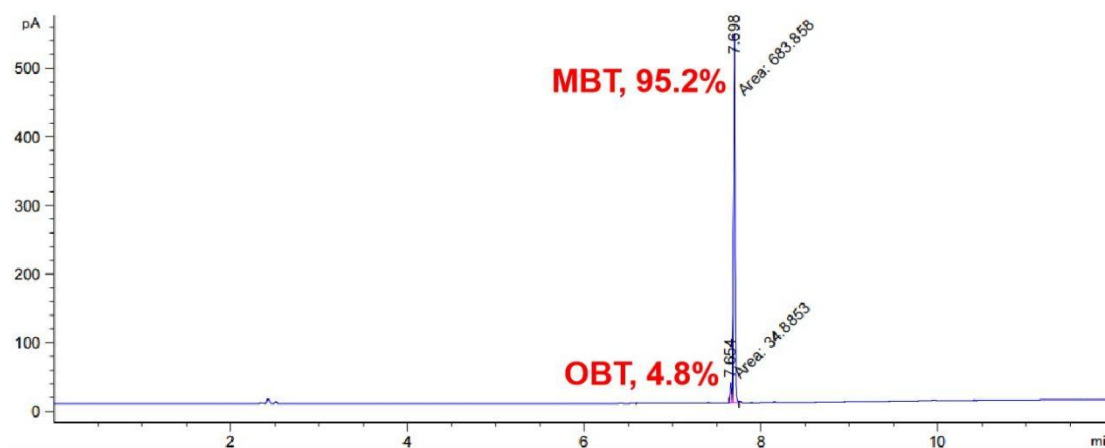


Fig. S32 The second cycle of adsorption of the equal volume mixture of **MBT** and **OBT** by **BrP5** crystals measured by GC.

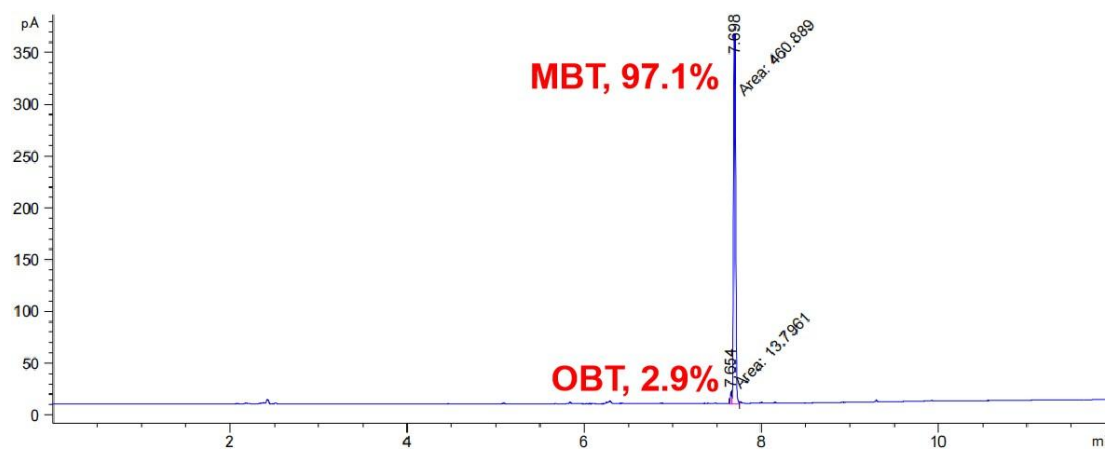


Fig. S33 The third cycle of adsorption of the equal volume mixture of **MBT** and **OBT** by **BrP5** crystals measured by GC.

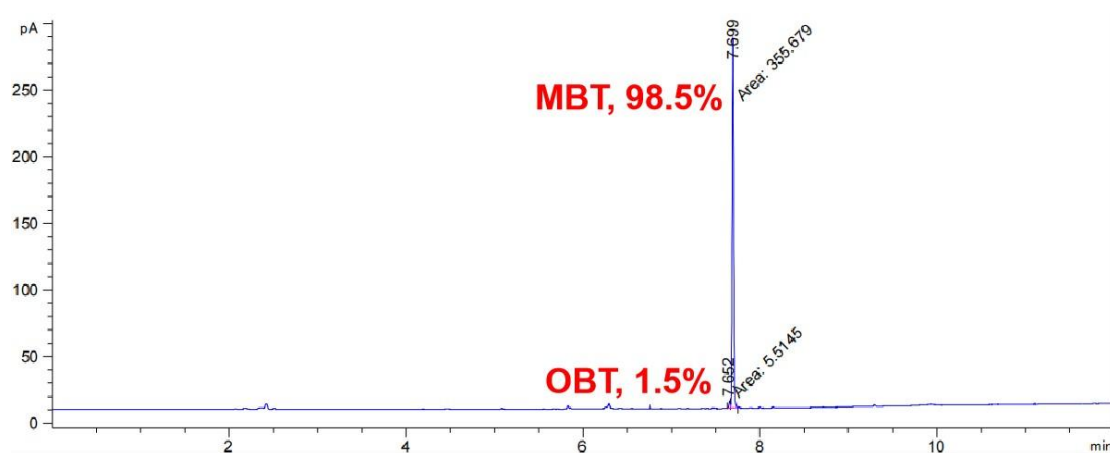


Fig. S34 The fourth cycle of adsorption of the equal volume mixture of MBT and OBT by BrP5 crystals measured by GC.

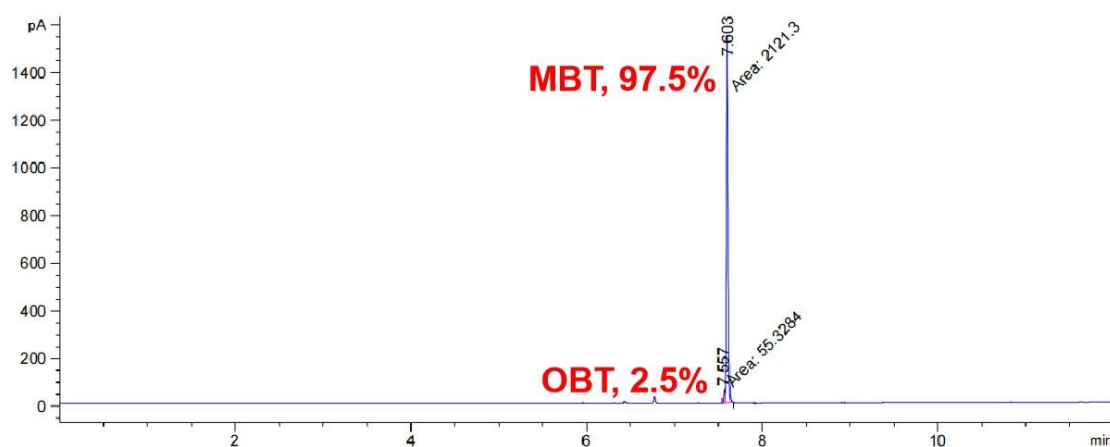


Fig. S35 The fifth cycle of adsorption of the equal volume mixture of MBT and OBT by BrP5 crystals measured by GC.

7. References

S1 Y. Yao, M. Xue, X. Chi, Y. Ma, J. He, Z. Abliz and F. Huang, *Chem. Commun.*, 2012, **48**, 6505–6507.

S2 Y. Yao, J. Li, J. Dai, X. Chi and M. Xue, *RSC Adv.*, 2014, **4**, 9039–9043.

S3 E. Li, Y. Zhou, R. Zhao, K. Jie and F. Huang, *Angew. Chem. Int. Ed.*, 2019, **58**, 3981–3985.

S4 S. Fang, E. Li, D. Zhu, G. Wu, Q. Zhang, C. Lin, F. Huang and H. Li, *Chem. Commun.*, 2021, **57**, 6074–6077.